

Magnetic emittance suppression using a bucking coil for a dc photocathode electron gun

Ryoji Nagai, Ryoichi Hajima, and Nobuyuki Nishimori

Citation: *Review of Scientific Instruments* **83**, 123303 (2012); doi: 10.1063/1.4772397

View online: <http://dx.doi.org/10.1063/1.4772397>

View Table of Contents: <http://scitation.aip.org/content/aip/journal/rsi/83/12?ver=pdfcov>

Published by the [AIP Publishing](#)

Articles you may be interested in

[High-voltage testing of a 500-kV dc photocathode electron gun](#)

Rev. Sci. Instrum. **81**, 033304 (2010); 10.1063/1.3354980

[Low Emittance Electron Gun for XFEL Application](#)

AIP Conf. Proc. **1149**, 1104 (2009); 10.1063/1.3215602

[Initial Emittance Measurements for Polarized Electron Gun with NEA-GaAs Type Photocathode](#)


AIP Conf. Proc. **915**, 1071 (2007); 10.1063/1.2750955

[Radio-frequency photocathode guns triggered by free electron laser light](#)

J. Appl. Phys. **93**, 641 (2003); 10.1063/1.1525859

[Photocathode electron gun applications in research and industry](#)

AIP Conf. Proc. **576**, 615 (2001); 10.1063/1.1395384



Nanopositioning Systems Micropositioning AFM & SPM Single molecule imaging

Magnetic emittance suppression using a bucking coil for a dc photocathode electron gun

Ryoji Nagai,^{a)} Ryoichi Hajima, and Nobuyuki Nishimori
 Japan Atomic Energy Agency (JAEA), Tokai, Ibaraki 319-1195, Japan

(Received 18 September 2012; accepted 1 December 2012; published online 20 December 2012)

Magnetic emittance suppression was demonstrated using a bucking coil for a dc photocathode electron gun. The magnetic emittance is derived from a leakage magnetic field on the cathode surface originating from a solenoid lens, and is important for realizing a high brightness dc photocathode electron gun. In order to solve this problem, a bucking coil integrated solenoid lens has been developed. The solenoid lens consists of a main coil, a bucking coil, and a pure iron yoke. The bucking coil and the main coil are integrated in the same yoke in order to prevent distortion of the magnetic field due to misalignment of the two coils. The emittance was measured and calculated as a function of the exciting current of the bucking coil and as a function of the electron beam size on the cathode.

© 2012 American Institute of Physics. [<http://dx.doi.org/10.1063/1.4772397>]

I. INTRODUCTION

An energy-recovery linac (ERL) which is a new class of electron accelerator is considered as a promising device for next-generation light sources, such as high-power free-electron lasers,^{1,2} next-generation X-ray light sources,³ high-flux γ -ray sources,^{4,5} and high-power THz sources.⁶ The ERL has the advantage that the emittance of the electron bunch generated by the electron gun is maintained for a light source, because another fresh electron bunch is accelerated at every turn. To exploit the full potential of the ERL, the most important component is the electron gun, which produces ultra-small emittance electron bunches with a high-average current.

The emittance of the beam generated by the dc electron gun consists of thermal emittance, emittance growth due to space charge forces, and magnetic emittance. The thermal emittance is due to the effective thermal energy of the electrons in the photocathode. An electron gun equipped with a semiconductor photocathode having a negative electron affinity (NEA) surface⁷ is known to have a naturally low thermal emittance. Thus, NEA photocathode dc electron guns are under development for ERLs in many laboratories.⁸⁻¹¹

The emittance growth due to space charge forces can be compensated for by using a solenoid lens.¹² Because the compensation is not effective if the solenoid lens is placed too far from the cathode, the solenoid lens has to be placed near the cathode. However, this leads another increase of emittance by a leakage magnetic field on the cathode from the solenoid lens. The emittance increase is known as “magnetic emittance,” according to Busch’s theorem.¹³ To achieve a zero magnetic field on the cathode surface, a bucking coil has typically been used with high brightness electron guns.^{14,15} However, to the best of our knowledge, the performance of a bucking coil has not been demonstrated.

In the present study, a bucking coil integrated solenoid lens was developed for a dc photocathode electron gun developed at the Japan Atomic Energy Agency (JAEA) in order to

demonstrate the suppression of magnetic emittance. A large bore size for the solenoid lens was employed in order to expand the misalignment tolerance. The solenoid lens consists of a main coil, a bucking coil, and a pure iron yoke. The bucking coil and the main coil are integrated in the same yoke in order to prevent distortion of the magnetic field due to misalignment of the two coils. Herein, we present the results of our attempt to suppress the magnetic emittance, and details of the design and performance of the solenoid lens.

II. MAGNETIC EMITTANCE AND BUCKING COIL

The total emittance of the electron beam ε_{total} generated by a dc photocathode gun consists of thermal emittance, emittance growth due to space charge forces, and magnetic emittance, and is presented by

$$\varepsilon_{total} = \sqrt{\varepsilon_{th}^2 + \varepsilon_{SC}^2 + \varepsilon_{mag}^2}, \quad (1)$$

where ε_{th} is the thermal emittance, ε_{SC} the emittance growth due to space charge forces, and ε_{mag} is the magnetic emittance. Because the considered beam is generated by a dc photocathode gun, the rf emittance is not contained.

The thermal emittance ε_{th} is known to be given by

$$\varepsilon_{th} = \sigma \sqrt{\frac{k_B T}{m_e c^2}}, \quad (2)$$

where σ is the root mean square (rms) size of the electron beam on the cathode, $k_B T$ is the effective thermal energy of the initial electron, m_e is the rest mass of the electron, and c is the speed of light. In the case of an NEA photocathode, the effective thermal energy is in the range of several tens of meV.²³ The emittance growth due to space charge force can be compensated for by using a solenoid lens placed in a suitable position.

The magnetic emittance originates from the leakage magnetic field on the cathode, which comes from the solenoid

^{a)}nagai.ryoji@jaea.go.jp.

lens. The magnetic emittance ε_{mag} is given by²²

$$\varepsilon_{mag} = \sigma^2 \frac{e|B_{z0}|}{2m_e c}, \quad (3)$$

where e is the elementary electric charge and B_{z0} is the leakage magnetic field on the cathode surface. The magnetic emittance becomes zero if the leakage magnetic field on the cathode is made zero by using a bucking coil in the solenoid lens. For example, with an electron beam size of 1 mm, in order to suppress the magnetic emittance to less than 1% of the thermal emittance corresponding to a thermal energy of 40 meV, the leakage magnetic field has to be less than 0.14 mT.

III. DESIGN AND PERFORMANCE OF THE SOLENOID LENS

In order to suppress the magnetic emittance by using a bucking coil, a bucking coil integrated solenoid lens was developed for a 250-kV dc photocathode electron gun,¹⁶ which is a testing machine for photocathodes intended for next-generation light sources. The solenoid lens consists of a main coil, a bucking coil, and a pure iron yoke. The main coil and bucking coil are made of a conventional hollow conductor with a cross-sectional size of $8 \times 8 \text{ mm}^2$ with a $4 \times 4 \text{ mm}^2$ cooling water hole. The large bore size was employed for expansion of the misalignment tolerance. The bucking coil and the main coil were integrated in the same yoke in order to prevent distortion of the magnetic field due to misalignment of the two coils. One of the required performance features of the solenoid lens is the generation of a sufficient peak magnetic field in order to compensate for the emittance growth due to the space charge forces. With an electron beam energy of 250 kV, the required peak field is approximately 30 mT, as estimated using the particle tracking code Paramela.¹⁷ Another required performance feature of the solenoid lens is the achievement of a zero magnetic field on the cathode surface. To reduce the leakage magnetic field from the main coil on the surface of the cathode, the shape of the yoke, as shown in Fig. 1, was employed. The leakage magnetic field of the main coil is suppressed by the reverse magnetic field of the bucking coil.

The performance of the solenoid lens was evaluated by measuring and calculating the field distribution. The field

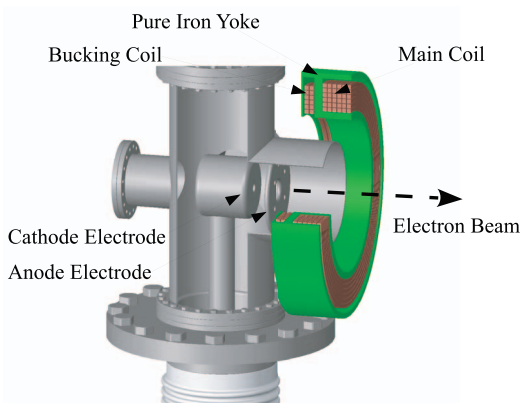


FIG. 1. 3D-CAD drawing of the solenoid lens.

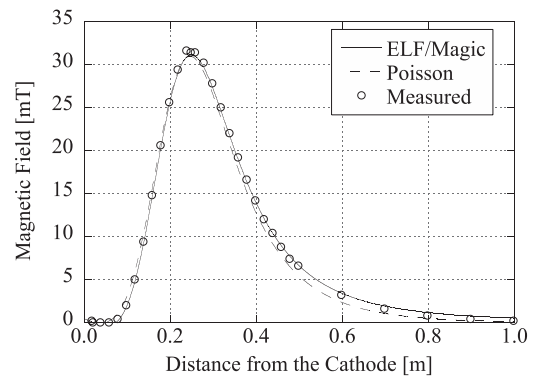


FIG. 2. Magnetic field distributions as a function of the distance from the cathode. The open circles show the measured values, and the solid and dashed lines represent the results calculated using the ELF/magic and Poisson codes, respectively.

measurement was achieved using a hole probe and linear motion stages. The field calculation was completed using the numerical computation codes, ELF/Magic¹⁸ and Poisson.¹⁹ When the main coil current was set at 280 A and the bucking coil current was adjusted such that there was a zero magnetic field on the cathode surface, the measured and calculated magnetic field distributions of the beam axis were determined, as shown in Fig. 2. The peak magnetic field is approximately 31 mT, and the peak magnetic field position was located in approximately 25 cm from the cathode. The measured magnetic field distribution is in good agreement with the calculated field distribution. The optimal current of the bucking coil as a function of the main coil current is shown in Fig. 3(a). The calculated results differ between the two codes because the calculation methods differ. ELF/Magic and Poisson calculate the magnetic field using the modified integral

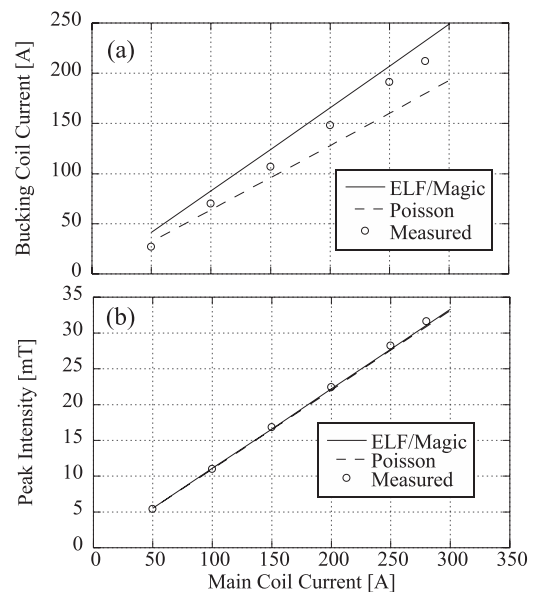


FIG. 3. Bucking coil exciting currents on which the leakage magnetic field on the cathode surface depend (a) and the peak magnetic field intensities (b) as a function of the exciting current of the main coil. The solid and dashed lines represent the results calculated using the ELF/magic and Poisson codes, respectively. The open circles represent the measured values.

element method and the conventional finite element method, respectively. The measured results are in good agreement with both results. The good linearity between the exciting current of the main coil and the peak magnetic field intensity, as seen in Fig. 3(b), indicates that the magnetic field is not saturated in the yoke.

IV. DEMONSTRATION OF THE MAGNETIC EMITTANCE SUPPRESSION

A. Emittance measurement

The magnetic emittance suppression was demonstrated through emittance measurements of the dc photocathode electron gun. The exciting current of the bucking coil was measured for the 250-kV photocathode electron gun. The electron gun is equipped with a GaAs photocathode that has an NEA surface. A GaAs wafer with $1.3 \times 10^{19} \text{ cm}^{-3}$ Zn doping was activated in the preparation chamber of the load-lock system connected to the gun. The quantum efficiency of the NEA-GaAs photocathode was 0.3% at 633 nm (He-Ne laser) during the emittance measurements. An adjustable telescope was used to illuminate a Gaussian profile laser beam onto the cathode. The laser profile was equal to the electron beam size on the cathode surface. The electron beam size on the cathode surface was then changed from 0.1350 mm to 1.076 mm. The following beam parameters were selected in order to clearly compare the thermal emittance with the magnetic emittance, when the space charge forces were negligible: a beam energy of 180 keV and a current of less than $1 \mu\text{A}$.

The emittance measurement apparatus was installed directly after the gun (see Fig. 4). The apparatus consisted of a moving slit, a screen monitor, and a Faraday cup. The geomagnetic field around the apparatus was degaussed using Helmholtz coils. The Faraday cup was placed just behind the screen monitor in order to measure the beam current. The emittance was measured using a single slit method.²⁰ A $50 \mu\text{m}$ wide slit made of tungsten was placed 1.13 m downstream from the cathode. At the slit position, the leakage magnetic field of the solenoid lens was less than 0.02 mT. A 0.1 mm thick aluminum-coated Ce:YAG scintillator was used for the screen, and the distance between the slit and the screen was 1.40 m. The beam profile image on the screen was observed with a charge-coupled device (CCD) camera interfaced to a data gathering computer. The single slit method provides

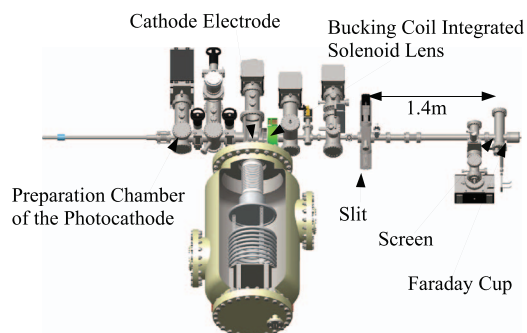


FIG. 4. 3D-CAD drawing of the emittance measurement setup.

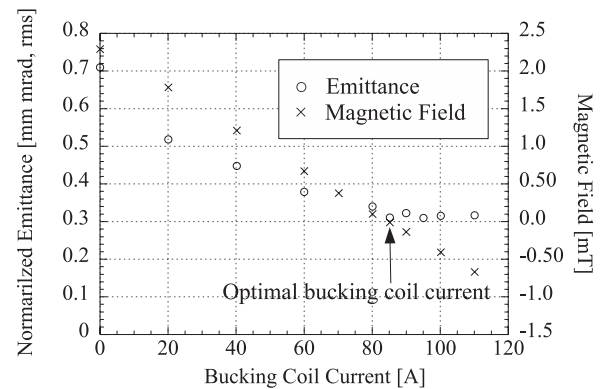


FIG. 5. Measured emittance and measured leakage magnetic field on the cathode surface as a function of the exciting current of the bucking coil. The open circle and crosses represent the emittance and leakage field, respectively.

a phase space intensity map of the electron beam. The slit scans the range of approximately 6.5 mm in $70 \mu\text{m}$ steps in about 7 min. Noise and background subtraction are important when calculating the rms emittance using the phase space intensity map. The phase space map is then analyzed using the “self-consistent, unbiased elliptical exclusion method.”²¹

The bucking coil current dependence of the emittance of the electron beam was measured with a main coil current of 105 A and an electron beam size on the cathode of 1.076 mm (see Fig. 5). To minimize the scan range of the slit, the main coil current was adjusted such that the electron beam was focused near the slit. The electron beam size on the cathode was at a maximum in this measurement setup in order to clarify the influence of the magnetic emittance. The emittance decreased as the exciting current of the bucking coil increased, and reached a minimum value of 0.311 mm mrad at an exciting current of 85 A. The leakage magnetic field on the cathode surface was measured using a hole probe located at the cathode position. The leakage magnetic field also decreased as the bucking coil exciting current increased, and vanished at an exciting current of 85 A. This result corresponds to the emittance measurement result.

The magnetic emittance is proportional to the square of the rms size of the electron beam on the cathode, as shown in Eq. (3). On the other hand, the thermal emittance is proportional to the electron beam size (see Eq. (2)). If the magnetic emittance is suppressed completely, the measured emittance is thus proportional to the electron beam size. The dependence of the emittance on the electron beam size was measured with zero current and an optimal current of 85 A for the bucking coil. As shown in Fig. 6, with a bucking coil current of 85 A, the dependence of the emittance on the electron beam size is linear. This behavior indicates that the magnetic emittance is suppressed completely. The effective thermal energy was evaluated from the slope of the line passing through the origin and fitted to the emittance versus the electron beam size. An effective thermal energy of 41.6 meV at a wavelength of 633 nm was obtained and is in good agreement with the previous measurement by Dunham *et al.*²³ When the bucking coil current was zero, the dependence of the emittance on the

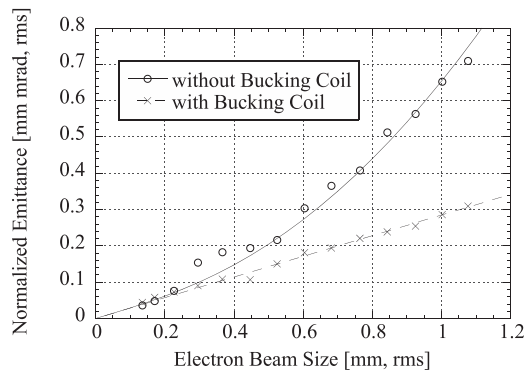


FIG. 6. The measured emittance with a zero exciting current and the optimal current for the bucking coil as a function of the electron beam size on the cathode. The open circles and crosses represent the emittance with a zero exciting and the optimal exciting current, respectively. The solid and dashed lines represent the fitting of the measured emittance versus the laser spot size with the zero exciting and optimal exciting currents, respectively.

electron beam size was not linear. This result indicates that magnetic emittance occurs due to the leakage magnetic field on the cathode surface. The leakage magnetic field was evaluated by fitting to the emittance as a function of the electron beam size, and was found to be 2.0 mT, which is in a good agreement with the measured value using a hole probe (see Fig. 5).

B. Numerical calculations

To verify the measurement results, the emittance at the slit position was evaluated by numerical calculation using the simulation code Paramela. The acceleration electric field distribution of the electron gun and the magnetic field distribution of the solenoid lens were calculated using Poisson and then used in the Paramela. Because the beam current was small enough during the measurements, the space charge effects were not calculated. Macro particles in the Paramela simulation were generated in a Gaussian transverse profile at the cathode position according to the illuminated laser profile on the cathode. The effective thermal energy of the macro particles was set to 41.6 meV at a transverse rms size of 0.2 mm.

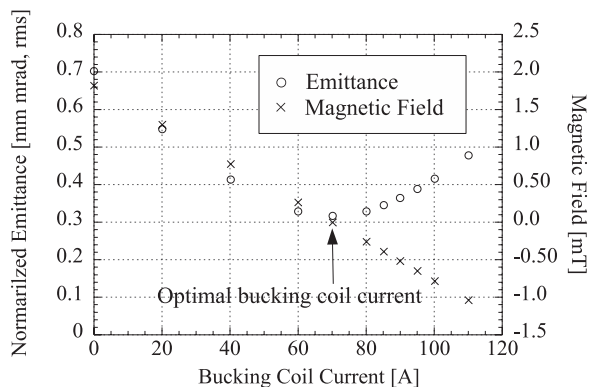


FIG. 7. Calculated emittance and leakage magnetic field on the cathode surface as a function of the exciting current of the bucking coil. The open circles and crosses represent the emittance and leakage field, respectively.

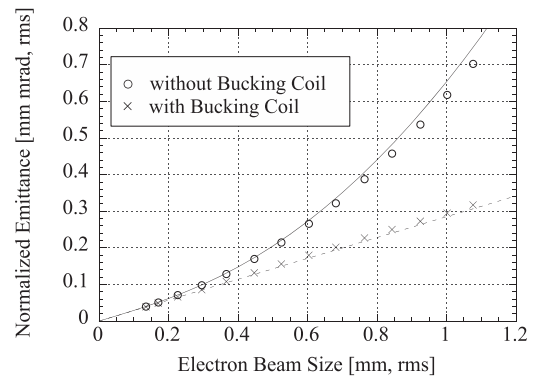


FIG. 8. The calculated emittance with a zero exciting current and the optimal current of the bucking coil as a function of the electron beam size on the cathode. The open circles and crosses represent the emittance with zero exciting and the optimal exciting currents, respectively. The solid and dashed lines represent the measured emittance fitting line with zero exciting and optimal exciting currents, respectively.

The bucking coil current dependence of the emittance of the electron beam was calculated under the same conditions as those used for the experimental measurement. As shown in Fig. 7, the emittance decreased as the exciting current of the bucking coil increased, and it reached a minimum value of 0.317 mm mrad at the bucking coil current of 70 A. The leakage magnetic field on the cathode surface was calculated using Poisson, and it was found that the leakage vanished at 70 A. The optimal current of the bucking coil is strongly dependent on the permeability characteristic of the yoke. The actual permeability characteristic of the yoke cannot fully be taken into account in the numerical calculation because the actual permeability characteristic changes with the history of the machining of the yoke. Therefore, the measured optimal current of the bucking coil differs from the calculated current. Although we have not investigated the behavior of the emittance beyond the optimal current, the calculated result that the emittance is minimized when there is a zero leakage magnetic field, which corresponds with the measurement of the dependence of the emittance on the bucking coil current. The relationship between the emittance and the electron beam size on the cathode was calculated with both the zero current and optimal current for the bucking coil excitation. Figure 8 shows that the calculated results are in good agreement with the measured values.

V. CONCLUSION

A bucking coil integrated solenoid lens was developed for the 250-kV photocathode dc electron gun¹⁶ at the JAEA. Magnetic emittance suppression using the bucking coil was demonstrated through measurement and calculation of the emittance of the dc photocathode electron gun. If the magnetic emittance is negligibly small, the thermal emittance is dominant and the total emittance is proportional to the electron beam size on the cathode. We verified the relationship between the emittance and the electron beam size with and without bucking coil excitation. The magnetic emittance is fully suppressed using the bucking coil. It was also found that adjustment of the bucking coil exciting current based on

the magnetic field calculation is insufficient, and adjustment based on analysis of the actual equipment is indispensable.

ACKNOWLEDGMENTS

The authors wish to thank Dr. T. Hayakawa of the JAEA for his encouragement and helpful discussions.

- ¹G. R. Neil, C. Behre, S. V. Benson, M. Bevins, G. Biallas, J. Boyce, J. Coleman, L. A. Dillon-Townes, D. Douglas, H. F. Dylla, R. Evans, A. Grippo, D. Gruber, J. Gubeli, D. Hardy, C. Hernandez-Garcia, K. Jordan, M. J. Kelley, L. Merminga, J. Mammoser, W. Moore, N. Nishimori, E. Pozdeyev, J. Preble, R. Rimmer, M. Shinn, T. Siggins, C. Tennant, R. Walker, G. P. Williams, and S. Zhang, *Nucl. Instrum. Methods Phys. Res. A* **557**, 9–15 (2006).
- ²E. J. Minehara, *Nucl. Instrum. Methods Phys. Res. A* **557**, 16–22 (2006).
- ³S. M. Gruner, D. Bilderback, and I. Bazarov, *Rev. Sci. Instrum.* **73**, 1402 (2002).
- ⁴R. Hajima, N. Kikuzawa, N. Nishimori, T. Hayakawa, T. Shizuma, K. Kawase, M. Kando, E. Minehara, H. Toyokawa, and H. Ohgaki, *Nucl. Instrum. Methods Phys. Res. A* **608**, S57–S61 (2009).
- ⁵V. N. Litvinenko, I. Ben-Zvi, E. Pozdeyev, and T. Roser, *IEEE Trans. Plasma Sci.* **36**, 1799 (2008).
- ⁶K. Harada, M. Shimada, and R. Hajima, *Infrared Phys. Technol.* **51**, 386–389 (2008).
- ⁷C. Hernandez-Garcia, T. Siggins, S. Benson, D. Bullard, H. F. Dylla, K. Jordan, C. Murray, G. R. Neil, M. Shinn, and R. Walker, in *Proceedings of 2005 Particle Accelerator Conference* (IEEE, Tennessee, 2005), pp. 3117–3119.
- ⁸K. Smolenski, I. Bazarov, B. Dunham, H. Li, Y. Li, X. Liu, D. Ouzounov, and C. Sinclair, *AIP Conf. Proc.* **1149**, 1077–1083 (2009).
- ⁹C. Hernandez-Garcia, S. V. Benson, G. Biallas, D. Bullard, P. Evtushenko, K. Jordan, M. Klopff, D. Sexton, C. Tennant, R. Walker, and G. Williams, *AIP Conf. Proc.* **1149**, 1071–1076 (2009).
- ¹⁰L. B. Jones, S. P. Jamison, Y. M. Saveliev, K. J. Middlemam, and S. L. Smith, *AIP Conf. Proc.* **1149**, 1084–1088 (2009).
- ¹¹N. Nishimori, R. Nagai, H. Iijima, Y. Honda, T. Muto, M. Kuriki, M. Yamamoto, S. Okumi, T. Nakanishi, and R. Hajima, *AIP Conf. Proc.* **1149**, 1094–1098 (2009).
- ¹²B. E. Carlsten, *Nucl. Instrum. Methods Phys. Res. A* **285**, 313–319 (1989).
- ¹³M. Reiser, *Theory and Design of Charged Particle Beams* (Wiley, 1994), p. 281.
- ¹⁴J. M. Maxson, I. V. Bazarov, K. W. Smolenski, and B. Dunham, in *Proceedings of 2011 Particle Accelerator Conference* (IEEE, New York, 2011), pp. 1945–1947.
- ¹⁵A. Hoffer, P. Evtushenko, and M. Krasilnikov, in *Proceedings of 2007 Particle Accelerator Conference* (IEEE, New Mexico, 2007), pp. 1326–1328.
- ¹⁶R. Nagai, H. Iijima, N. Nishimori, R. Hajima, T. Muto, Y. Honda, and T. Miyajima, in *Proceedings of 2009 Particle Accelerator Conference* (IEEE, British Columbia, 2009), pp. 545–547.
- ¹⁷L. M. Young, Los Alamos National Laboratory Report No. LA-UR-96-1835, Revised July 19, 2005.
- ¹⁸ELF Corporation, *ELF/Magic Reference Manual* (ELF Corporation, 1995).
- ¹⁹J. H. Billen and L. M. Young, Los Alamos National Laboratory Report No. LA-UR-96-1834, Revised June 28, 2005.
- ²⁰L. Staykov, “Characterization of the transverse phase space at the photoinjector test facility in DESY, Zeuthen site,” Ph.D. dissertation (Universität Hamburg, 2008).
- ²¹M. P. Stockli, R. F. Welton, and R. Keller, *Rev. Sci. Instrum.* **75**, 1646–1649 (2004).
- ²²D. T. Palmer, X. J. Wangy, I. Ben-Zviy, R. H. Miller, and J. Skaritka, in *Proceedings of 1997 Particle Accelerator Conference* (IEEE, British Columbia, 1998), pp. 2843–2845.
- ²³B. M. Dunham, L. S. Cardman, and C. K. Sinclair, in *Proceedings of 1995 Particle Accelerator Conference* (IEEE, Texas, 1996), pp. 1030–1032.